

Secondary Circulation in Fluid Flow

Author(s): W. R. Hawthorne

Source: *Proceedings of the Royal Society of London. Series A, Mathematical and Physical Sciences*, Vol. 206, No. 1086 (May 7, 1951), pp. 374-387

Published by: [The Royal Society](#)

Stable URL: <http://www.jstor.org/stable/98575>

Accessed: 18-08-2015 09:19 UTC

Your use of the JSTOR archive indicates your acceptance of the Terms & Conditions of Use, available at <http://www.jstor.org/page/info/about/policies/terms.jsp>

JSTOR is a not-for-profit service that helps scholars, researchers, and students discover, use, and build upon a wide range of content in a trusted digital archive. We use information technology and tools to increase productivity and facilitate new forms of scholarship. For more information about JSTOR, please contact support@jstor.org.



The Royal Society is collaborating with JSTOR to digitize, preserve and extend access to *Proceedings of the Royal Society of London. Series A, Mathematical and Physical Sciences*.

<http://www.jstor.org>

Secondary circulation in fluid flow

BY W. R. HAWTHORNE, SC.D.

Gas Turbine Laboratory, Massachusetts Institute of Technology

(Communicated by Th. von Kármán, For. Mem. R.S.—Received 24 June 1950—
Revised 13 October 1950)

Secondary circulation appears after fluid with a non-uniform velocity distribution passes round a bend. It alters the character of the flow and is a source of loss. A general expression is developed for its change along a streamline in a perfect, incompressible fluid.

The flow in bent circular pipes is analyzed and the theory is compared with experiments on bent pipes and rectangular ducts. In bends the secondary flow is not spiral but oscillatory, the direction of the circulation changing periodically.

The theory shows that secondary circulation remains unchanged if streamlines are geodesics on surfaces of constant total pressure.

INTRODUCTION

The existence of secondary currents in bends in pipes and rivers has been known for some time. James Thomson (1877) showed experimentally that a spiral flow could be obtained in a curved stream of water, the secondary motion at the bottom being inward and that at the top outward. The secondary flow was attributed to the effect of the centrifugal pressure gradient in the main flow acting on the relatively stagnant fluid in the wall boundary layer.

Theoretical analysis of secondary flows has almost entirely been confined to the work of Dean (1927) for laminar flow in pipe bends of large ratio of bend radius to pipe diameter. Recently, however, Squire & Winter (1949) showed that secondary flows could occur in a bend through which a perfect, i.e. inviscid, fluid is flowing, as a result of a non-uniform distribution of velocity at entrance to the bend. Squire & Winter's work, which will be referred to again, suggested that a more general theoretical investigation of the rotational flow of a perfect fluid in three dimensions might yield useful results, if attention was concentrated on the secondary circulation, or the component of vorticity in the direction of flow.

GENERAL THEORY

The theory will be presented for a steady, inviscid, incompressible fluid in motion in the absence of body forces. Representing the velocity vector by \mathbf{V} and its scalar by q , the vorticity vector

$$\boldsymbol{\Omega} = \text{curl } \mathbf{V}. \quad (1)$$

The component of the vorticity resolved in the direction of flow, whose scalar will be presented by ξ , gives rise to a secondary circulation which, when measured around a stream tube of cross-sectional area dA , has a magnitude $= \xi dA$. Since $q dA$ is the constant volume flow along a stream tube, the secondary circulation around any given stream tube will be proportional to ξ/q .

The vorticity may be resolved along and normal to a streamline to give

$$\left(\frac{\boldsymbol{\Omega} \cdot \mathbf{V}}{\mathbf{V} \cdot \mathbf{V}} \right) \mathbf{V} = \frac{\xi}{q} \mathbf{V} \quad \text{along a streamline,}$$

and $\frac{(\mathbf{V} \times \boldsymbol{\Omega}) \times \mathbf{V}}{(\mathbf{V} \cdot \mathbf{V})}$ normal to a streamline.

Since the divergence of the curl of a vector is zero,

$$\operatorname{div} \boldsymbol{\Omega} = 0. \tag{2}$$

Resolving the vorticity into its two components

$$\operatorname{div} \frac{\xi}{q} \mathbf{V} - \operatorname{div} \frac{\mathbf{V} \times (\mathbf{V} \times \boldsymbol{\Omega})}{(\mathbf{V} \cdot \mathbf{V})} = 0,$$

or, expanding,

$$\frac{\xi}{q} \operatorname{div} \mathbf{V} + \mathbf{V} \cdot \operatorname{grad} \frac{\xi}{q} - \mathbf{V} \times (\mathbf{V} \times \boldsymbol{\Omega}) \cdot \operatorname{grad} \frac{1}{\mathbf{V} \cdot \mathbf{V}} - \frac{1}{q^2} \operatorname{div} \mathbf{V} \times (\mathbf{V} \times \boldsymbol{\Omega}) = 0. \tag{3}$$

Now $\operatorname{div} \mathbf{V} \times (\mathbf{V} \times \boldsymbol{\Omega}) \equiv (\mathbf{V} \times \boldsymbol{\Omega}) \cdot \operatorname{curl} \mathbf{V} - \mathbf{V} \cdot \operatorname{curl} (\mathbf{V} \times \boldsymbol{\Omega})$ (4)

is an identity. The first term on the right-hand side contains two identical vectors $\boldsymbol{\Omega}$ and $\operatorname{curl} \mathbf{V}$ and is therefore zero, so that, if $\operatorname{curl} (\mathbf{V} \times \boldsymbol{\Omega})$ is zero, the entire right-hand side becomes zero.

For the type of flow specified the streamlines and vortex lines lie in a surface of constant total pressure p_0 , or a Bernoulli surface. It may be shown (Lamb 1932) that

$$\mathbf{V} \times \boldsymbol{\Omega} = \operatorname{grad} \frac{p_0}{\rho} = \operatorname{grad} \left(\frac{p}{\rho} + \frac{1}{2} q^2 \right); \tag{5}$$

consequently $\operatorname{curl} (\mathbf{V} \times \boldsymbol{\Omega}) = 0$.

The continuity relation is $\operatorname{div} \mathbf{V} = 0$; hence, the first and last terms in equation (3) disappear leaving

$$\mathbf{V} \cdot \operatorname{grad} \frac{\xi}{q} = \frac{-\mathbf{V} \times (\mathbf{V} \times \boldsymbol{\Omega}) \cdot \operatorname{grad} (\mathbf{V} \cdot \mathbf{V})}{q^4}. \tag{6}$$

Now $\operatorname{grad} (\mathbf{V} \cdot \mathbf{V}) \equiv 2(\mathbf{V} \cdot \nabla) \mathbf{V} + 2\mathbf{V} \times \operatorname{curl} \mathbf{V}$ (7)

is an identity, which when substituted in equation (6) yields

$$\mathbf{V} \cdot \operatorname{grad} \frac{\xi}{q} = - \frac{\mathbf{V} \times (\mathbf{V} \times \boldsymbol{\Omega}) \cdot 2(\mathbf{V} \cdot \nabla) \mathbf{V}}{q^4}. \tag{8}$$

Another form of this relation which may be derived by a similar procedure is

$$\operatorname{div} (\boldsymbol{\Omega} \cdot \mathbf{V}) \mathbf{V} = \operatorname{div} (\mathbf{V} \cdot \mathbf{V}) \boldsymbol{\Omega}, \tag{8a}$$

or $\mathbf{V} \cdot \operatorname{grad} (\boldsymbol{\Omega} \cdot \mathbf{V}) = \boldsymbol{\Omega} \cdot \operatorname{grad} (\mathbf{V} \cdot \mathbf{V}).$ (8b)

The left-hand side of equation (8) is proportional to the product of the velocity and the rate of change along a streamline of the secondary circulation. The triple product on the right-hand side of equation (8) is proportional to the product of the velocity, a vector $(\mathbf{V} \times \boldsymbol{\Omega})$ normal to the Bernoulli surface containing the streamline and hence normal to the velocity vector, and a vector representing the acceleration. The acceleration may be resolved into two components, one tangential to the streamline and the other along the principal normal. The acceleration along the principal normal is q^2/R , where $1/R$ is the curvature of the streamline. If ϕ is the

angle between the directions of the principal normal and the normal to the Bernoulli surface, then the only component of acceleration entering into the triple product is $\sin \phi \cdot q^2/R$, the other two components having the directions of $(\mathbf{V} \times \boldsymbol{\Omega})$ and \mathbf{V} .

Hence equation (8) becomes

$$\mathbf{V} \cdot \text{grad} \frac{\xi}{q} = -2 \frac{|\text{grad}(p_0/\rho)| \sin \phi}{q R}. \quad (9)$$

Integrating along a streamline

$$\left(\frac{\xi}{q}\right)_2 - \left(\frac{\xi}{q}\right)_1 = -2 \int_1^2 \frac{1}{q^2} \left| \text{grad} \left(\frac{p_0}{\rho}\right) \right| \frac{\sin \phi}{R} ds, \quad (10)$$

where ds is an elementary arc of the streamline.

Now $(\sin \phi/R) = (1/R_g)$, the geodesic curvature of the streamlines on the Bernoulli surface. The sign of the change in secondary circulation depends on the direction in which the streamline is turning away from the plane containing the vectors \mathbf{V} and $(\mathbf{V} \times \boldsymbol{\Omega})$. If the streamline turns towards the direction of the vortex lines, then the geodesic curvature (or ϕ) is negative; if away, ϕ is positive, the positive direction of the vorticity being determined by the usual right-hand screw rule.

By definition
$$\frac{1}{R} = \frac{d\theta}{ds},$$

where $d\theta$ is the angle between tangents to the streamline at points are length ds apart; hence equation (10) may also be written

$$\left(\frac{\xi}{q}\right)_2 - \left(\frac{\xi}{q}\right)_1 = -2 \int_1^2 \left| \text{grad} p_0/\rho \right| \sin \phi \frac{d\theta}{q^2}. \quad (11)$$

An important result of this analysis is that if $\phi = 0$ or the direction of acceleration (or pressure gradient) lies in the plane containing the velocity vector and the normal to the Bernoulli surface, there is no change in secondary circulation along the streamline. Hence streamlines along which the secondary circulation remains unchanged are geodesics on the Bernoulli surface.

SOME EXAMPLES SOLUBLE BY SUPERIMPOSITION

The simplest examples to which this analytical result may be applied are those in which the initial flow has a uniform pressure and a velocity varying in only one direction. Such a flow may exist in the boundary layer of a large straight duct or in an open channel whose width is large compared to its depth. The Bernoulli surfaces are planes and the total pressure varies in one direction only. If the stream enters a bend whose plane is parallel to the Bernoulli surfaces, the angle ϕ between the direction of normal acceleration and the normal to the Bernoulli surface is initially $\frac{1}{2}\pi$, so that a secondary circulation is created in the bend. Since each particle of perfect fluid retains its original total pressure and the particles are carried with the secondary flow, the Bernoulli surfaces are distorted as the fluid passes downstream so that the original unidirectional feature of the total pressure variation is lost.

Equation (11) is not sufficient to determine the flow, but if certain assumptions are made, approximate solutions may be obtained by estimating the secondary

vorticity. These assumptions are that the secondary flow occurs in planes which are normal to the average direction of flow, that the secondary vorticity is normal to these planes, and that the secondary flow may be treated as a two-dimensional plane flow superimposed on the main flow. To obtain the secondary vorticity from equation (11) the behaviour of the Bernoulli surfaces and streamlines must either be estimated or calculated by some step-by-step process.

In the flow of a boundary layer described above, the Bernoulli surfaces are initially planes and are distorted as the flow proceeds round the bend. Under certain conditions the distortion of the Bernoulli surfaces may be small, and $|\text{grad } p_0/\rho|$ and ϕ will retain their initial values. If the variation in q along a streamline is also small, and noting that initially

$$\text{grad } p_0/\rho = \text{grad } (p/\rho + \frac{1}{2}q^2) = q \text{ grad } q = q\Omega_0,$$

where Ω_0 is the initial vorticity, equation (11) gives for the vorticity downstream

$$\xi_2 = -2\Omega_0 \epsilon, \quad (12)$$

where ϵ is the angle of turn in the bend. These are the assumptions and the result obtained by Squire & Winter (1949) using a different analytical approach.

A similar method of superimposition may be used for the flow around an obstacle, such as an aerofoil, when the velocity varies only in the direction of the span. Then equation (11) yields for the downstream vorticity

$$\left(\frac{\xi}{q}\right)_2 = -2\Omega_0 q_0 \int_1^2 \frac{d\theta}{q^2}, \quad (13)$$

where the integral may be evaluated along a streamline of the unperturbed, i.e. two-dimensional flow around the obstacle. Equation (13) shows that a symmetrical obstacle such as a cylinder or strut will create a secondary vorticity due to its thickness alone. The secondary vorticity will result in induced drag effects which may be reduced by minimizing the integral in equation (13). This is a possible basis for a method of designing thick struts for use in boundary layers.

FLOW IN A BENT CIRCULAR PIPE

In many instances the distortion of the Bernoulli surfaces during the flow round the bend cannot be neglected. The following example shows how equation (11) may then be used to obtain approximate solutions. Suppose that an initial flow with uniform pressure and a velocity varying in one direction only enters a bent circular pipe of diameter d . The entry velocity and Bernoulli surfaces are shown in figure 1*a* and *b* respectively. If the plane of the bend is parallel to the initial Bernoulli surfaces, then ϕ is initially $\frac{1}{2}\pi$, and after a small turn in the bend a secondary circulation will appear in the direction shown by the arrow in figure 1*b*.

The secondary flow carries with it particles, identified by their total pressure, giving rise to a spiral motion in the bend. After a small turn in the bend the diagram showing the contours of total pressure over a cross-section of the pipe will no longer appear as in figure 1*b* but will be distorted in the direction of the arrow as a result of the spiral flow.

As a first approximation it will be assumed that the distortion of the contours of total pressure is a simple twist of the diagram through an angle α to give the picture shown in figure 1c. If this happens, the normal to the Bernoulli surfaces will have turned through the angle α , but the normal acceleration of the fluid will be still directed approximately towards the centre of the bend. Hence, the angle ϕ , which is initially $\frac{1}{2}\pi$, now will be $(\frac{1}{2}\pi - \alpha)$, and this value may be substituted in equation (11) giving

$$\frac{\xi}{q} = -2 \int_0^\theta |\text{grad } p_0/\rho| \cos \alpha \frac{d\theta}{q^2}. \tag{14}$$

Assuming that either ξ is uniform over the cross-section or that a suitable mean value may be defined whose product with the cross-sectional area of the pipe gives the total circulation, the clockwise circumferential velocity v at the outer diameter of the pipe is given by

$$v = -\frac{1}{4}\xi d. \tag{15}$$

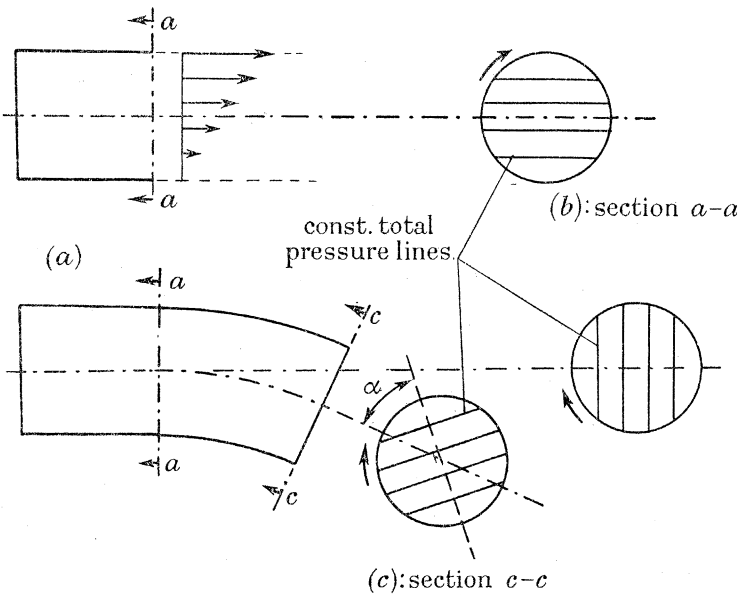


FIGURE 1. The effect of a bend on flow with a velocity gradient in a circular pipe. In (a) the surfaces of constant total pressure are horizontal planes as shown in (b). At section c-c these planes have turned through angle α (c).

The ratio of this circumferential velocity v to the velocity normal to the cross-section of the pipe, which is approximately q , gives the ratio of the linear displacements of a particle in the secondary- and main-flow directions. In an elementary turn of angle $d\theta$ in the bend, the angular displacement in the secondary-flow direction, using the notation of figure 1c, will be $d\alpha$. The linear displacements are approximately the products of $d\theta$ with r , the radius from the centre of the bend to the particle, and of $d\alpha$ with $\frac{1}{2}d$ the radius of the pipe. Hence

$$\frac{\frac{1}{2}d d\alpha}{r d\theta} = \frac{v}{q} = \frac{d}{2} \int_0^\theta \frac{|\text{grad } p_0/\rho|}{q^2} \cos \alpha d\theta. \tag{16}$$

Equation (16) may be solved readily if the bracketed term in the integral can be evaluated. For the simplified scheme shown in figure 1 in which the maximum velocity is U_m , the minimum zero and the velocity gradient is linear, initially

$$\frac{\text{grad } p_0/\rho}{q^2} = \frac{1}{q} |\text{grad } q| = \frac{U_m}{qd}. \tag{17}$$

If this term and the velocity q remain unchanged on any streamline, then by equation (14) the vorticity is uniform over the cross-section and the use of equation (15) is justifiable. To measure the turning the easiest particles to follow are those of highest total pressure, so that U_m may be substituted for q in equation (17) and $r = (R + \frac{1}{2}d \sin \alpha)$, where R is the radius of the bend to the centre of the pipe (pipes bent on a circular arc are assumed).

Substitution in (16) and the differentiation with respect to θ yields

$$\frac{1}{\left(\frac{2R}{d} + \sin \alpha\right)} \frac{d^2\alpha}{d\theta^2} - \frac{\cos \alpha}{\left(\frac{2R}{d} + \sin \alpha\right)^2} \left(\frac{d\alpha}{d\theta}\right)^2 = \frac{1}{2} \cos \alpha,$$

or

$$\frac{1}{\frac{2R}{d} + \sin \alpha} \frac{d}{d\alpha} \left(\frac{d\alpha}{d\theta}\right)^2 - \frac{2 \cos \alpha}{\left(\frac{2R}{d} + \sin \alpha\right)^2} \left(\frac{d\alpha}{d\theta}\right)^2 = \cos \alpha. \tag{18}$$

Since $(d\alpha/d\theta) = 0$ when $\theta = 0$, integration of this gives

$$\frac{d\alpha}{d\theta} = \left(\frac{2R}{d} + \sin \alpha\right) \left[\log_e \left(1 + \frac{d}{2R} \sin \alpha\right) \right]^{\frac{1}{2}}. \tag{19}$$

If R is large compared to the pipe diameter, equation (16) becomes approximately

$$\left(\frac{d}{R}\right) \frac{d^2\alpha}{d\theta^2} = \cos \alpha, \tag{20}$$

which is analogous to

$$\left(\frac{L}{g}\right) \frac{d^2\alpha}{dt^2} = \cos \alpha, \tag{21}$$

the equation of motion of a pendulum of length L making an angle α with the horizontal.

Hence the fluid in the bend will oscillate between $\alpha = 0$ and $\alpha = \pi$ with a period or bend deflexion for a complete oscillation approximately equal to $2\pi/\sqrt{(R/d)}$. The secondary circulation which is analogous to the kinetic energy of the pendulum will also oscillate with the same period, passing through zero after each $\pi \sqrt{(d/R)}$ radians of turn, approximately.

Equations (16) and (17) show that particles with smaller velocities than U_m have larger values of $(d\alpha/d\theta)$ and therefore tend to overtake the particles of higher total pressure. The assumption that the Bernoulli surfaces merely twist is, hence, only an approximation, as is the use of the largest total pressure particles to describe the average motion of the surfaces. Any alterations in the value of the bracketed term in the integral of equation (16) due to these effects or to the effects of friction, such as a decrease in the total pressure gradient, change the value of the period, as well as the magnitude of the secondary circulation.

EXPERIMENTS WITH CIRCULAR PIPE BENDS*

Tests were made by connecting circular pipes of about 6 in. inside diameter to a ventilating fan. The total pressure at inlet to the bent pipe was adjusted by means of screens of varying thickness to give an approximately linear velocity gradient. Two pipe bends were used, one of $6\frac{3}{8}$ in. inside diameter, a deflexion of 90° , and radius $9\frac{9}{16}$ in. giving $R/d = 1.5$. The other was 6 in. inside diameter, 180° deflexion, and radius 30 in. giving $R/d = 5$. The only measurements were of total pressure, obtained by pointing a pitot tube, $\frac{1}{8}$ in. outside diameter, in the direction which gave a maximum reading. To avoid the necessity for cutting holes in the pipe, the bends and straight pipes were cut so that Pitot tube surveys were always made at the outlet cross-section, successive sections of pipe being added to get readings further downstream.

Results from the 90° bend are shown in figure 2 as lines of constant total pressure on cross-sections at inlet and outlet from the bend and after straight pipes of varying lengths downstream. At outlet from the bend the Bernoulli surfaces have turned so that the particles of maximum total pressure have twisted through an angle of about 110° towards the outside of the bend. The predicted tendency for the particles of lower total pressure to twist more rapidly than those of higher total pressure is demonstrated by the crowding of total pressure lines at the top of section 2, figure 2, and their separation at the bottom. This is a partial explanation for the subsequent motion of the lower total pressure streamlines towards the centre of the pipe shown in sections 3 to 6, figure 2. The results are shown in table 1. Good agreement between theory, equation (19), and experiment at station 2 indicates the small effect of friction in the bend, confined mostly to the wall boundary layer. Other effects of friction are shown by a decrease in the rate of twist, $d\alpha/dx$, in the straight pipe downstream and a tendency for the total pressures to become more uniform, although the general stream pattern remains clear. The overall tendency of the low-velocity fluid originally on the bottom wall to move to the centre of the pipe is remarkable.

TABLE 1

station	2	—	3	4	5	6
distance, x (in.)	0	—	16	44	60	94
α (degrees)	110	(113)*	240	440	550	730
twist, $d\alpha/dx$ (degrees/in.)	9.2	(9.3)*	—	—	—	5.0

* Figures in parentheses are solutions of equation (19). Reynolds number based on maximum velocity = 200,000.

The results of the tests on the 180° bend $R/d = 5$ are shown in figures 3, 4 and 5. Figure 3 illustrates the test procedure and the total pressure contours at inlet to the bend. Pitot traverses were made every 30° of bend, and after a section of straight pipe 25 in. long placed downstream of each 30° section of the bend. The total pressure contours are shown in figure 4. Below that obtained after each 30° section is placed the corresponding contour after 25 in. of straight pipe. In this way the displacement

* The experiments described in this section were done by Hans P. Eichenberger, Dipl.Ing.ETH, graduate student at the Massachusetts Institute of Technology, whose help and comments are acknowledged.

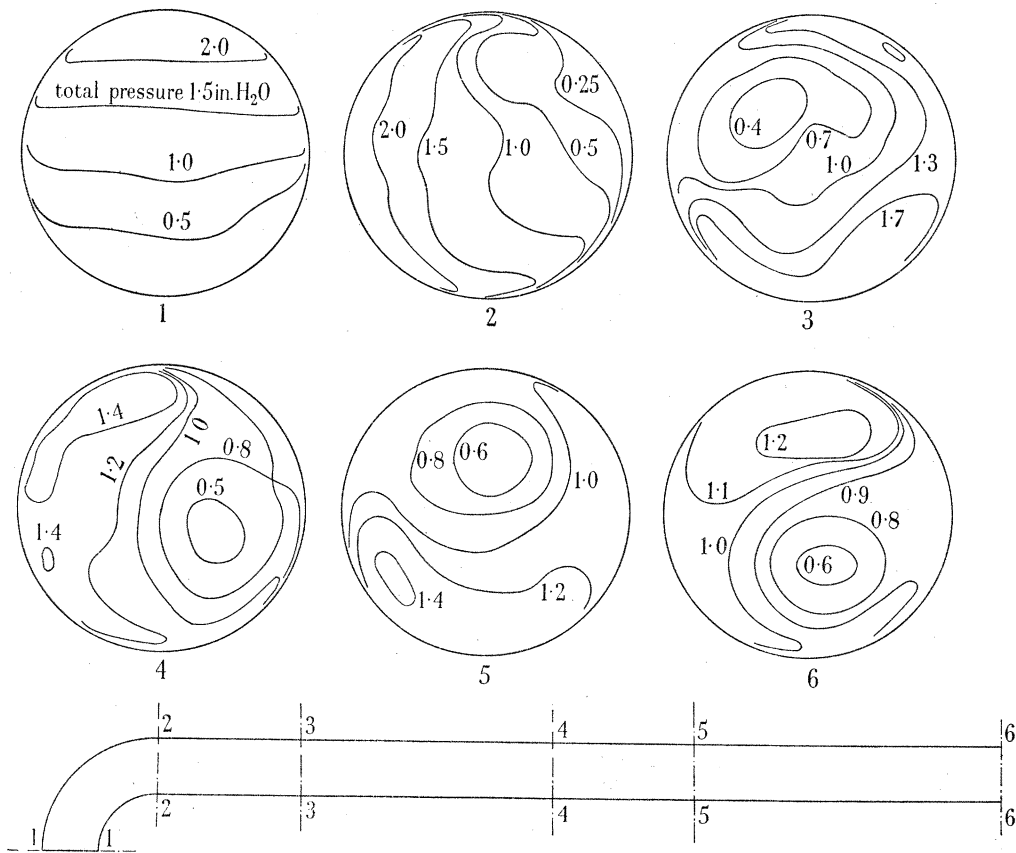


FIGURE 2. Results from 90° bend tests. $R/d = 1.5$, $d = 6\frac{3}{8}$ in.

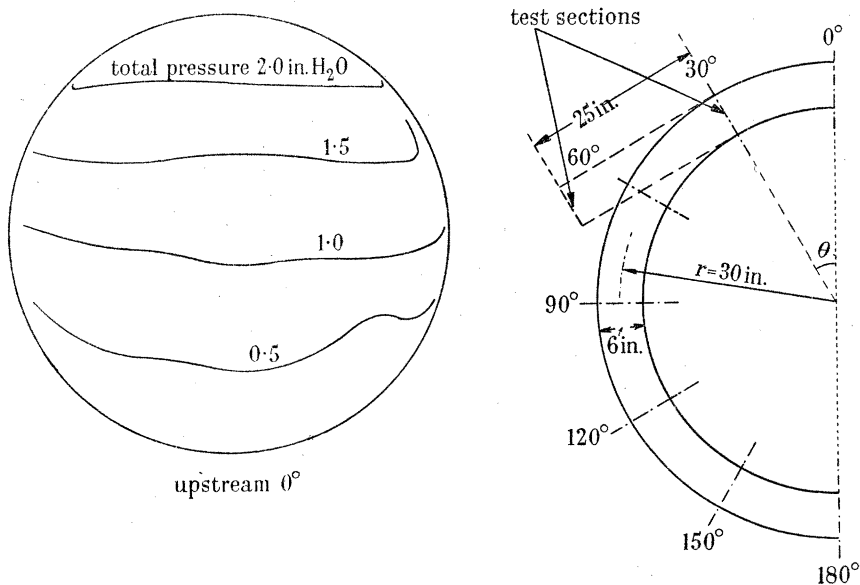


FIGURE 3. Test procedure used on bent circular pipe, $R/d = 5$ and inlet total pressure distribution.

and rate of turning were measured every 30° of bend. Figure 4 shows that the circulation is anti-clockwise up to 90° and then becomes clockwise from 120 to 180° . The total pressure contours remain nearly parallel lines, to some extent justifying the use of the simplified theory of the previous section. The oscillations of the fluid in the bend are shown in figure 5, which summarizes the results by showing the angular displacement as $(\frac{1}{2}\pi - \alpha)$ and the secondary circulation as twist per 25 in.

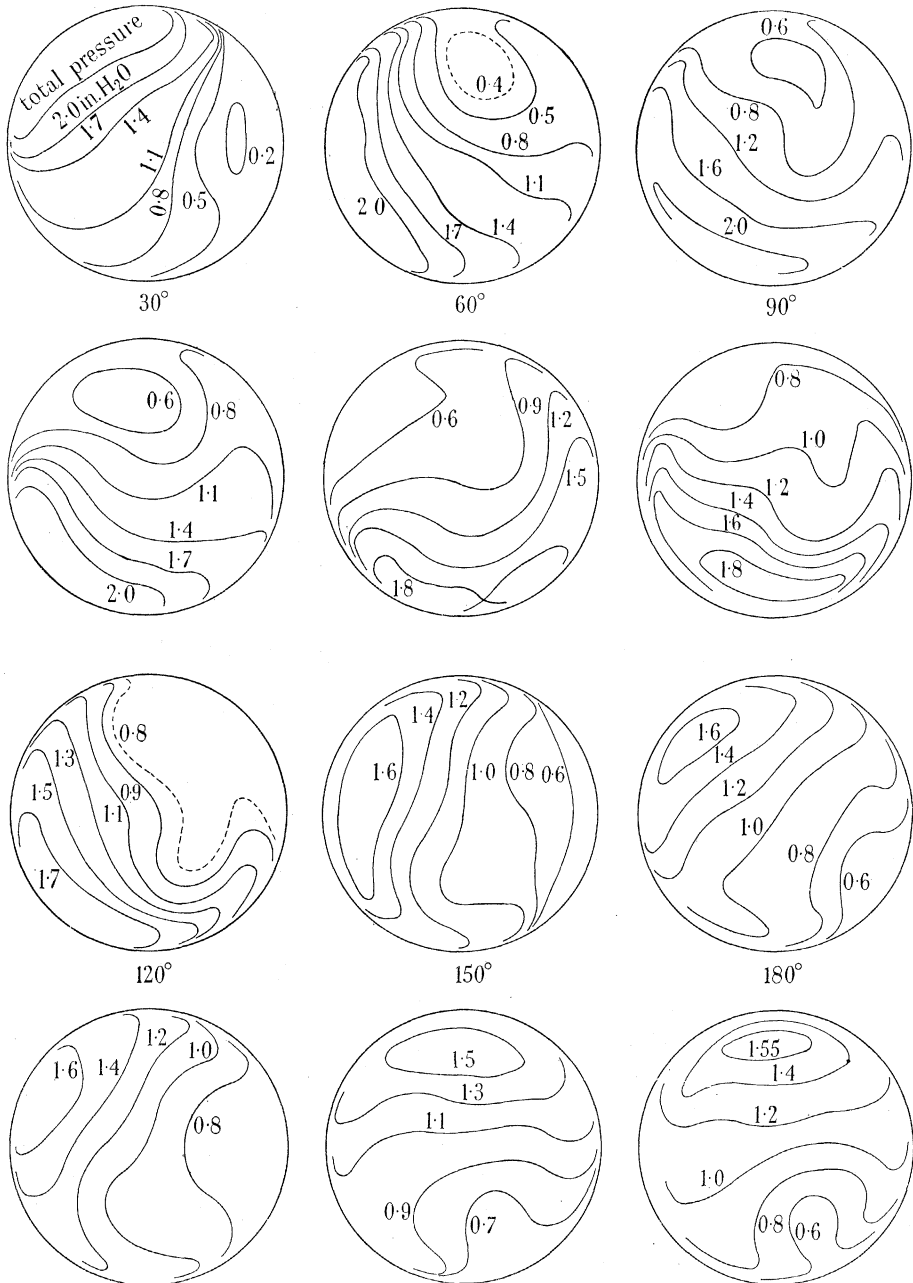


FIGURE 4. Results of tests on bent circular pipe, $R/d = 5$. Sections every 30° of bend with, below, sections taken after 25 in. of straight pipe.

of straight pipe, both measurements referred to the particles of highest total pressure. The solution of equation (19) is the broken curve shown in figure 5.

Although the damping effect of friction on the oscillation is large, there is qualitative agreement with the simplified inviscid fluid theory. To obtain closer agreement with experiment, the theory can be modified. Allowance for wall friction accounts for most of the change in amplitude of the displacement. The differing rates of twisting of the various streamlines tend to decrease the period and the decrease of the total pressure gradient from its initial value tends to increase it.

While the initial shear flow is the result of viscous effects, it is of interest that friction in the bend reduces rather than promotes the secondary circulation.

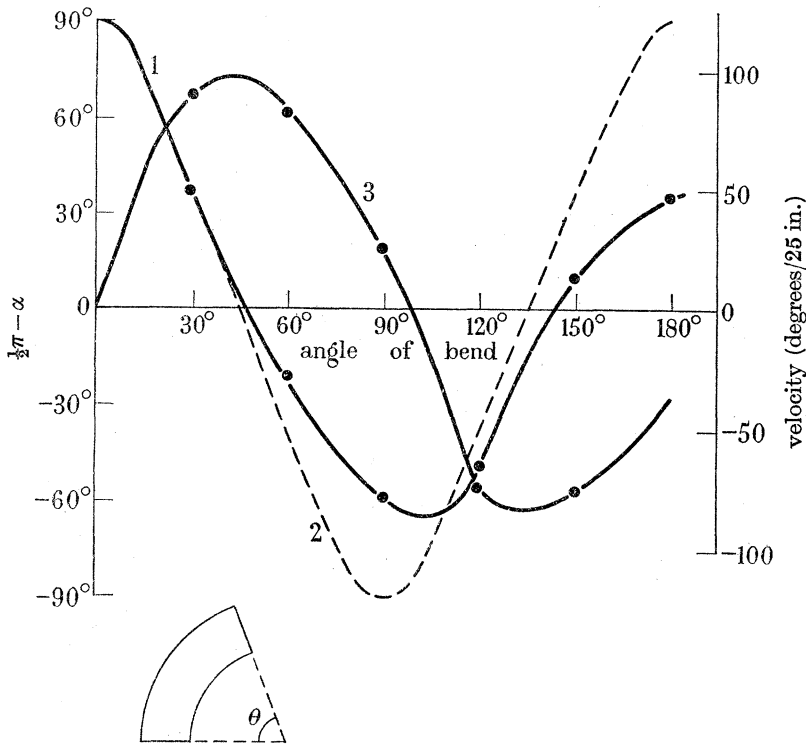


FIGURE 5. Effect of deflexion on displacement and turning rate of highest total pressure particles in circular pipe bend, $R/d = 5$. Curve 1, measured turning angle α ; curve 2, calculated α ; curve 3, velocity of turning.

EXPERIMENTS WITH RECTANGULAR BENDS

Similar tests were made by W. Joy (1950) with a bent rectangular duct 5 in. \times 10 in. The total pressure at inlet was adjusted to give the symmetrical velocity distributions shown in figure 6. Three constant radius bends were used; one of 7 in. radius to the centre line and 90° deflexion, both the others were of 15 in. radius, one being of 90° and the other of 180° deflexion. The 10 in. long side of the rectangular section was perpendicular to the plane of the bend. Total pressures were measured with a Pitot tube inserted through slots in the wall at various sections of the bend and the

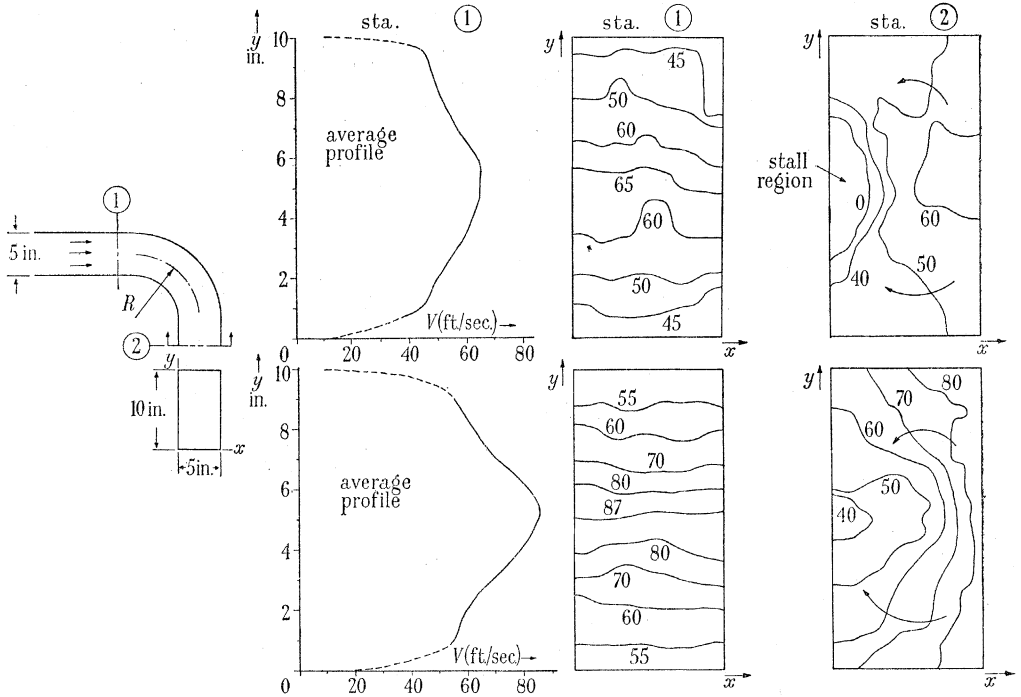


FIGURE 6. Velocity distributions in 90° bend of 5 × 10 in. rectangular duct; bend radii: top, 7 in.; bottom, 15 in.

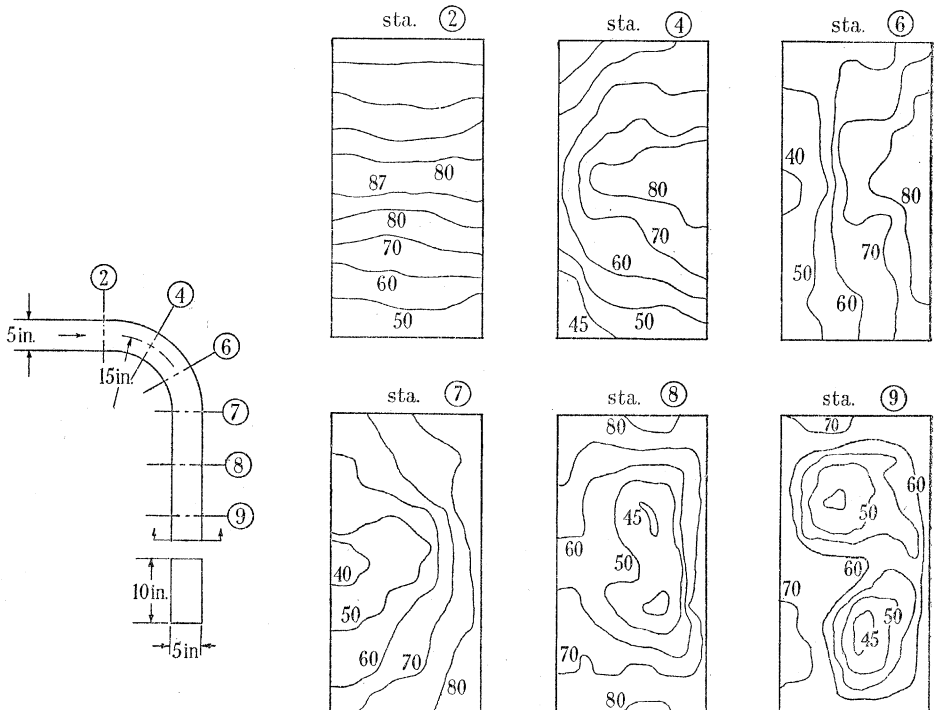


FIGURE 7. Velocity (ft./sec.) distributions in 90° bend of 5 × 10 in. duct; bend radius 15 in. at various stations in the bend, 30° apart, and in a straight duct downstream, 12 in. apart.

straight duct downstream. Static pressures were measured with wall taps. The results shown in figures 6, 7 and 8 are given as velocity contours, but the effect of static pressure is so small that the total pressure contours practically coincide with them.

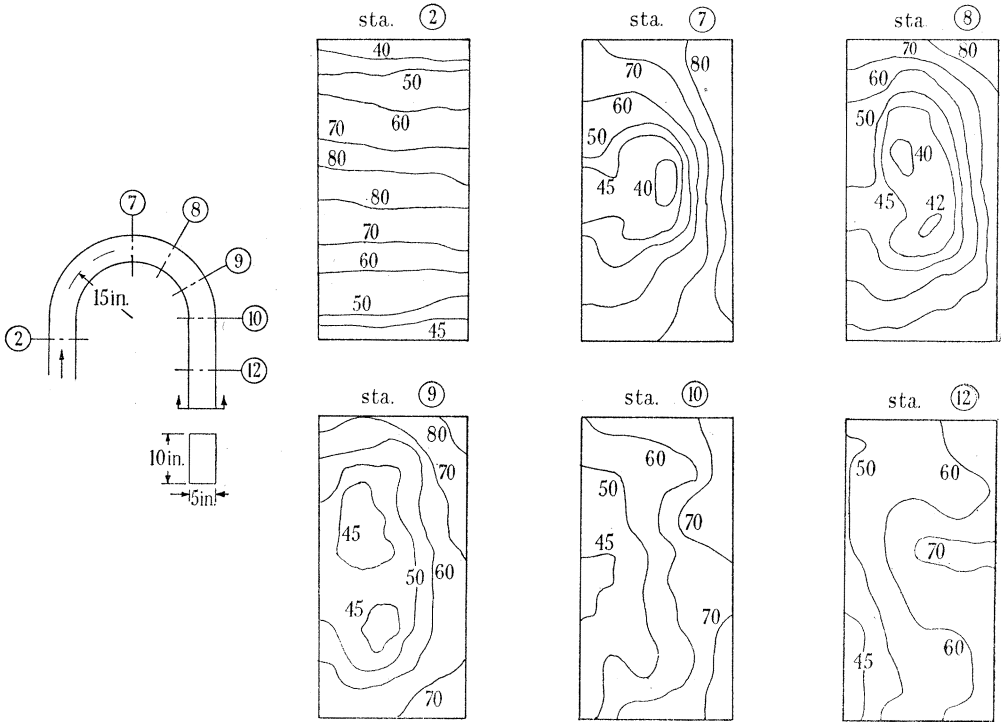


FIGURE 8. Velocity distributions in 180° bend of 5 × 10 in. duct; bend radius 15 in. at various stations in the bend, 30° apart, and downstream, 12 in. apart. Direction of secondary flow reverses at station 8.

As the fluid moves around the bend, the Bernoulli surfaces move from a horizontal to a vertical position, each pair joining up and the higher total pressure particles moving towards the outside of the bend, figure 7. After further deflexion the surfaces of the higher total pressure close round the fluid of low total pressure, station 7, figure 8. The fluid of higher total pressure continues to rotate pushing the low total pressure fluid until it separates into two regions located roughly at the centres of the top and bottom halves of the duct, station 8, figure 8. If the bend continues, the direction of the circulation changes, station 9, figure 8, and the surfaces of total pressure return towards their original positions, station 10, figure 8. The configuration of the fluid in the duct downstream develops from the point in the cycle at which the bend terminates. The fluid originally on the top and bottom walls finally appears downstream in two 'islands' in the centre of each half of the duct, figure 7.

The effect of bend radius is shown in figure 6. After 90° deflexion the Bernoulli surfaces have twisted further in the 15 in. bend than in the 7 in. bend.

Analyzed by a simple inviscid fluid theory similar to that given for the circular pipe, an agreement between experiment and theory nearly as good as that for the circular pipe is obtained.

DISCUSSION

A comparison between reported measurements of pressure losses in pipe bends reveals considerable variation in the loss coefficients obtained by different investigators. Furthermore, as the bend radius ratio is changed, keeping the deflexion constant, the bend loss coefficient varies in an almost periodic fashion. Results of tests on a 90° bend by Davis (1910) are shown in figure 9. It is possible that these variations are due to the oscillatory changes in the secondary circulation discovered here. The discrepancies between the results of different investigators are probably due to differing velocity distributions at inlet to the bend.

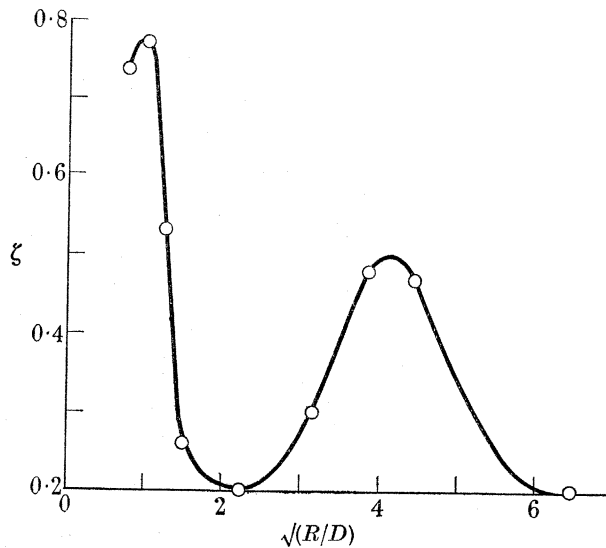


FIGURE 9. The effect of bend radius on the loss coefficient ζ , in excess of that in straight pipe for 90° circular pipe bends. After Davis (1910).

Although frictional effects become important in the flow downstream of the bend, any discussion would consider first the inviscid fluid theory. In the inviscid fluid theory if, as is plausible, there is no further change in secondary circulation in the downstream flow, then the streamlines must be geodesics on the stream surfaces. Limiting consideration to this type of flow, it may be shown that if the flow conditions do not vary in the downstream directions, i.e. the components of $\text{grad } p$, etc., in the downstream direction are zero, then the Bernoulli surfaces are circular cylinders, coinciding with the surfaces of constant pressure and constant velocity and the streamlines are helices. If the flow conditions show a pattern which remains unchanged except in orientation, resembling somewhat the results at stations 4, 5 and 6 of figure 2, then the Bernoulli surfaces coincide with surfaces of constant pressure and velocity. These results may be readily obtained, since in both types of flow the directions of $\text{grad } p$ and $\text{grad } p_0$ must coincide.

The general relation for the change in secondary circulation along a streamline may also be of particular interest in meteorology and in flow in rivers. It may offer some insight into the behaviour of boundary layers and the phenomena of transition from laminar to turbulent flow.

REFERENCES

- Davis, G. J. 1910 *Bull. Univ. Wis. Engng Series*, 6, no. 4.
 Dean, W. R. 1927 *Phil. Mag.* 4, 208.
 Joy, W. 1950 Thesis, Massachusetts Institute of Technology.
 Lamb, Sir Horace 1932 *Hydrodynamics*, 6th ed. p. 244. Cambridge University Press.
 Squire, H. B. & Winter, K. G. 1949 *R.A.E. Rep. Aero* 2317.
 Thomson, J. 1877 *Proc. Roy. Soc.* 26, 356.

The aerodynamic drag of a free water surface

BY J. R. D. FRANCIS
Imperial College, London

(Communicated by R. A. Bagnold, F.R.S.—Received 21 October 1950—
 Revised 15 December 1950—Read 15 March 1951)

The drag exerted by wind on a water surface has been measured in a tunnel 7.5 cm. wide and 7 m. long in which winds up to 14 m./sec. can be made. The waves thus formed are similar to those seen at sea. A device increases the effective fetch and therefore the size of the waves. The drag is measured by the slope of the mean water surface. The shear-stress coefficient $\gamma_a^2 = \tau/\rho u_a^2$ increases nearly linearly with wind speed, and the drag therefore increases nearly with the cube of the speed. There is a not unsatisfactory agreement with field results of shear coefficient, when the wind velocity is extrapolated to the greater height at which it is usually measured over the sea. It is thought that this agreement between the drag of small laboratory waves and large field waves may show that the mechanism for drag is not controlled by the wave size or speed, but perhaps by the tiny wind ripples.

The variation of wind speed with height has been measured. The profiles sometimes show anomalies in the zone up to about 8 cm. above the crests, there being slow layers of air between faster ones. The height of the anomalous zone increases as the waves become higher. Above 8 cm. the usual rough boundary law holds good. An empirical law is given for the shear stress as a function of the speed of the surface layer of water.

1. INTRODUCTION

When the wind blows over the sea, waves form on the water surface, and the drag slows the air immediately above to form a boundary layer. The conditions near the interface are important because they affect the transfer of heat and water vapour in the atmosphere, and the wave characteristics are of interest to the oceanographer, sailor and engineer. Of these boundary measurements the variation of wind speed with height above the sea has been investigated by Wust, Shoulejkin, Montgomery, N. K. Johnson, Roll, Sutcliffe and Bruch; and the slope of the mean sea surface caused by the drag has been measured by Palmen, Ekman, Hela and Corkan. There is, however, a large scatter in the values of the shear-stress coefficients $\gamma_a^2 = \tau/\rho u_a^2$ found in these field experiments, where τ = shear stress, ρ = air density, u_a = wind speed at height a above mean water-level. There are several possible reasons for the uncertainty: the difficulties of operating instruments of the necessary precision from small boats in rough seas; the tidal and seiche movements of the whole body of water masking the slope caused by the drag; the rarity of